Pergamon
www.elsevier.com/locate/asr
Available online at www.sciencedirect.com
SCIENCE DIRECT
doi: 10.1016/S0273-1177(03)00020-6

INTERNATIONAL REFERENCE IONOSPHERE 2000: EXAMPLES OF IMPROVEMENTS AND NEW FEATURES

D. Bilitza

Raytheon ITSS, NSSDC, GSFC, Code 632, Greenbelt, Maryland 20771, USA

ABSTRACT

This paper describes the changes that were implemented in the new version of the COSPAR/URSI International Reference Ionosphere (IRI-2000). These changes are: (1) two new options for the electron density in the D-region, (2) a better functional description of the electron density in the E-F merging region, (3) inclusion of the F1 layer occurrence probability as a new parameter, (4) a new model for the bottomside parameters B_0 and B_1 that greatly improves the representation at low and equatorial latitudes during high solar activities, (5) inclusion of a model for foF2 storm-time updating, (6) a new option for the electron temperature in the topside ionosphere, and (7) inclusion of a model for the equatorial F region ion drift. The main purpose of this paper is to provide the IRI users with examples of the effects of these changes.

INTRODUCTION

The International Reference Ionosphere (IRI) is a widely used standard for the specification of ionospheric parameters and is recommended for international use by the Committee On SPAce Research (COSPAR) and the International Union of Radio Science (URSI), e.g., at the 1999 URSI General Assembly in Toronto, Canada, the "URSI Commission G resolved that IRI be internationally recognized as the standard for the ionosphere." IRI was developed and is being improved/updated by a joint working group of URSI and COSPAR. The objectives are described in the terms of reference of the working group: (1) The task group was established to develop and improve a standard model of the ionospheric plasma parameters (electron and ion densities, temperatures, and velocities). The model should be primarily based on experimental evidence using all available ground and space data sources; theoretical considerations can be helpful in bridging data gaps and for internal consistency checks. (2) Where discrepancies exist between different data sources, the IRI team should promote critical discussion to establish the reliability of the different data bases. (3) IRI should be updated as new data become available and as old databases are fully evaluated and exploited.

The working group consists of a team of experts representing different countries, different measurement techniques, and different modeling groups. Currently, the roster includes 43 scientists from 17 countries: M. Abdu (Brazil), J. Adeniyi (Nigeria), A. Alcayde (France), D. Anderson (USA), K. Bibl (USA), D. Bilitza (USA, Chair), P. Bradley (UK), A. Danilov (Russia), V.K. Depuev (Russia), P. Dyson (Australia), R. Ezquer (Argentina), M. Friedrich (Austria), T. Fuller-Rowell (USA), T. Gulyaeva (Russia), S. Gupta (India), R. Hanbaba (France), X. Huang (USA), K. Igarashi (Japan), G. Ivanov-Kholodny (Russia), E. Kazimirovsky (Russia), P. Kishcha (Russia-Israel), E. Kopp (Switzerland), I.

Adv. Space Res. Vol. 31, No. 3, pp. 757–767, 2003

Printed in Great Britain
0273-1177/03 $30.00 + 0.00

Kutiev (Bulgaria), K. Mahajan (India), L.-A. McKinnell (South Africa), A. Mikhailov (Russia), A. Mitra (India), M. Mosert de Gonzalez (Argentina), K. Oyama (Japan,Vice-Chair COSPAR), A. Poole (South Africa), S. Pulinets (Russia), S. Radicella (Italy-Argentina), K. Rawer (Germany), B. Reinisch (USA,Vice-Chair URSI), M. Rycroft (UK), W. Singer (Germany), J. Sojka (USA), I. Stanislavska (Poland), L. Triskova (Czech Republic), V. Truhlik (Czech Republic), B. Ward (Australia), S. Watanabe (Japan), V. Wickwar (USA), P. Wilkinson (Australia), and B. Zolesi (Italy).

Progress of the various improvement efforts is discussed during annual IRI workshops. Papers from these meetings are published in Advances in Space Research. The special focus of the 1999 workshop at the University of Massachusetts Lowell was the description of ionospheric variability and ray tracing through model ionospheres (Rawer et al., 2001). The emphasis of the 2000 (COSPAR) session in Warsaw, Poland was on "Modeling the Topside Ionosphere and Plasmasphere" (Rawer et al., 2002). Since 1994 an annual IRI Task Force Activity (TFA) is being organized by S. Radicella at the International Center for Theoretical Physics (ICTP) in Trieste, Italy. The TFA has resulted in several improvements of the bottomside electron density profile that are included in IRI-2000 (Radicella, 2001, 2002; Radicella et al., 1998). The TFA focus has now shifted to the topside ionosphere and to quantitative descriptions of ionospheric variability (monthly quartiles).

Summary reports from the IRI meetings and general information about the IRI project are available from the IRI homepage at http://nssdc.gsfc.nasa.gov/space/model/ionos/iri.html. An IRI Newsletter is published quarterly (K. Oyama, editor). Information about model updates is also provided through an electronic mailer (see IRI home page). The newest version of the model, IRI-2000, was described and presented by Bilitza (2001). The IRI Fortran software can be retrieved via anonymous ftp from nssdc.gsfc.nasa.gov in directory pub/models/ionospheric/iri/iri2001 or using the URL ftp://nssdcftp.gsfc.nasa.gov/models/ionospheric/iri/iri2001/. This article provides examples of the various changes.

D REGION ELECTRON DENSITY

The lowest region (D region) is characterized by large variability and a very small database. The only data source are rocket experiments, because the region is too low for satellites and the densities are too low for ground ionosondes and radars. IRI 2000 includes two new options for the description of D region electron densities, reflecting the large uncertainties that still exist in this region. Option 1 is the current D region model that was developed by Mechtley and Bilitza (1974) (see also Bilitza, 1981) on the basis of a rather limited set of representative rocket data.

Option 2 is the model by Friedrich et al. (2000). Friedrich and Torkar (1998) have compiled a database of the most reliable D region rocket data (~200 profiles) and experimented with different modeling approaches, always including the strong dependence on solar zenith angle and considering to various degrees dependencies on season, latitude, solar activity, and neutral density and even an extension to high latitudes (Friedrich and Torkar, 1995). Their most recent modeling concept (Friedrich et al, 2000, Friedrich and Torkar, 2001) combines the rocket data with the results of a theoretical model. The model is exclusively based on reliable rocket data and exists as a number of tabulated profiles. Model profiles are obtained by suitably interpolating using the user-specified zenith angle, latitude, season, and solar activity.

Option 3 is the model of Danilov et al. (1995) that provides users with an estimate of the changes observed in the D region during disturbed conditions for winter daytime conditions. Although their rocket database is quite limited in volume, they find that the data can be grouped into five distinct classes using the following criteria: (1) undisturbed conditions, (2) weak winter anomaly (WA) defined by an increase of the absorption in the 2-2.8 MHz range at short A3 paths by 15 dB, (3) strong WA defined by an increase of 30 dB, (4) weak stratospheric warming conditions defined by a temperature increase at the 30 hPa level by 10 degrees, and (5) strong stratospheric warming conditions defined by an increase of 20 degrees. Temperature data for post-event analysis can be found in the "Beilage zur Berliner Wetterkarte" published by Karin Labitzke and her group.

An example of daytime D region profiles obtained with the different options in winter is shown in Figure 1. All models exhibit the characteristic inflection point at about 80 km that marks the transition from molecular to cluster ions. In our example the predictions of the Danilov-Rodevich-Smirnova model (Option 3) and the Mechtley-Bilitza model (Option 1) are close together at this altitude whereas the Friedrich-Torkar model differs by about a factor of 2. In accordance with observational evidence IRI-2000 allows WA and SW conditions only during winter. Figure 1 shows that a "Strong WA" can result in an increase of a factor of 10 at 80 km and a "Strong SW" in a decrease of about a factor of 2 at 80 km.

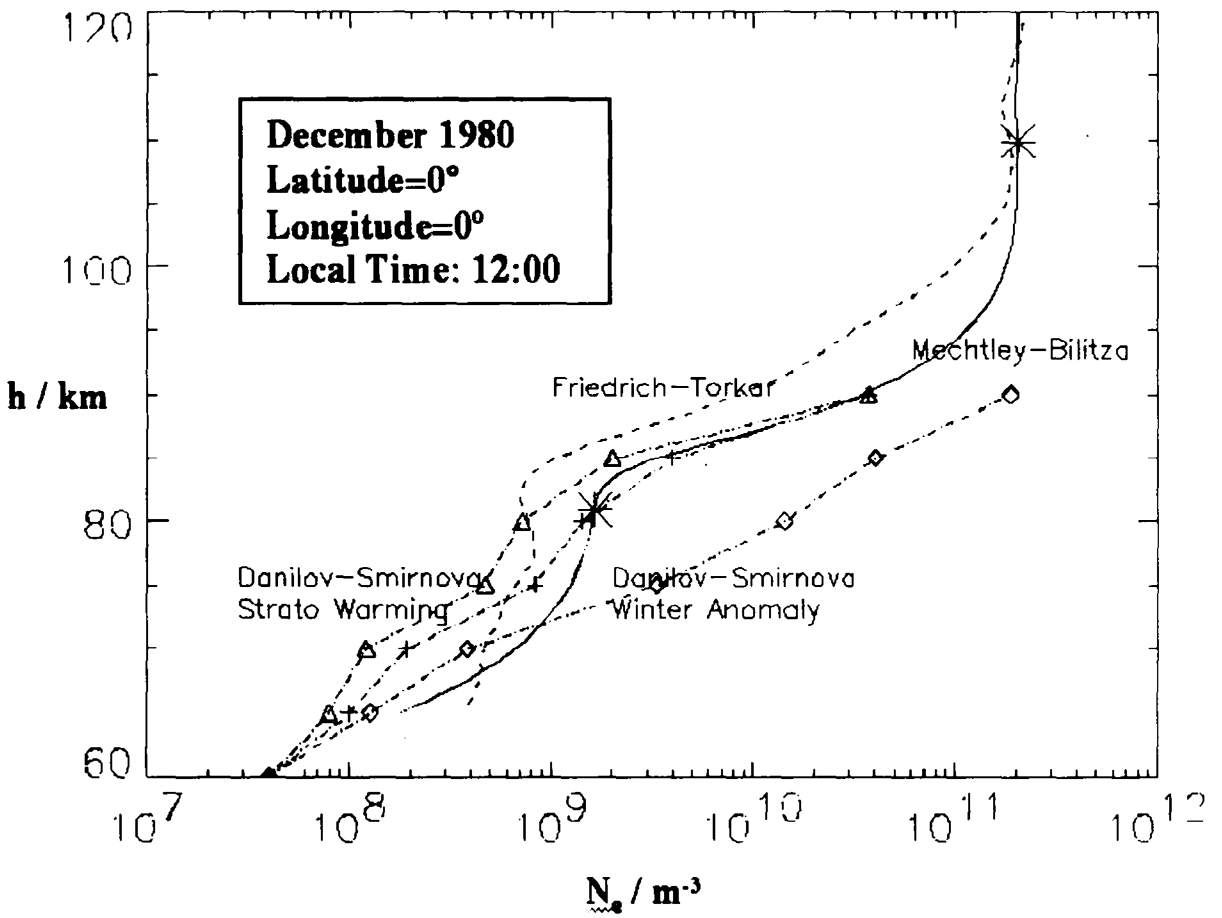

Fig. 1. The three IRI options for the D-region electron density for winter daytime conditions: Mechtley and Bilitza (1974) [solid line], Friedrich and Torkar (2001) [broken line], and Danilov et al. (1995) [dotted line] for conditions of stratospheric warming [triangles] and for Winter Anomaly [diamonds].

IMPROVED FUNCTIONAL DESCRIPTION OF TRANSITION REGION

The IRI electron density profile in the F region is normalized to the F peak density and height and in the E region to the E peak density and height. A merging algorithm is used to join the two profile parts. This transition region extends from the top of the E valley to the bottom of the F1 layer. The current formalism could lead to discontinuities or artificial valleys under conditions when merging was particularly difficult to accomplish, because of large differences between E and F peak densities and/or small differences between the E and F peak heights. A better functional description for the merging region was developed by Reinisch and Huang (1999). The new algorithm overcomes these problems and provides a much better representation of profile shapes observed by ionosondes as shown in Figure 2 in a comparison with measurements from the ionosonde at Ougadougou, Burkina Faso, near the magnetic equator. The formulas for the IRI bottomside profile (N_2), F1 region (N_3), and transition region (N_4), are

$$N_2(h)/NmF2 = \exp\{-x^{B1}\}/\cosh\{x\}, \quad x = (hmF2 - h)/B_0 \qquad (1)$$

$$N_3(h) = N_2(h^*), \quad h^* = hmF1 \cdot \{1 - ((hmF1-h)/hmF1)^{1+D1}\} \qquad (2)$$

$$N_4(h) = N_3(h^{**}), \quad h^{**} = h \qquad \text{if } h_{st} = h_{vt}, \qquad (3a)$$

$$h^{**} = h_z + T/2 - \{T\cdot(T/4-[h-h_z])\}^{1/2} \qquad \text{if } h_{st} > h_{vt} \qquad (3b)$$

$$h^{**} = h_z + T/2 + \{T\cdot(T/4-[h-h_z])\}^{1/2} \qquad \text{if } h_{st} < h_{vt} \qquad (3c)$$

$$T = (h_z - h_{st})^2/(h_{st} - h_{vt}), \quad h_z = (hmF1 + h_{st})/2 \qquad (3d)$$

where NmF2 is the density at the F2 peak, hmF2 is the F2 peak height, hmF1 the F1 peak height, h_{vt} is the height at the top of E valley, and h_{st} is the height where the bottomside function reaches the E peak density NmE (i.e., $N_3(h_{st})$ = NmE). The F1 layer shape factor D_1 varies with modified dip latitude (in the same way as in the previous version of IRI, called C_1 then) and with local time using a simple cosine dependence.

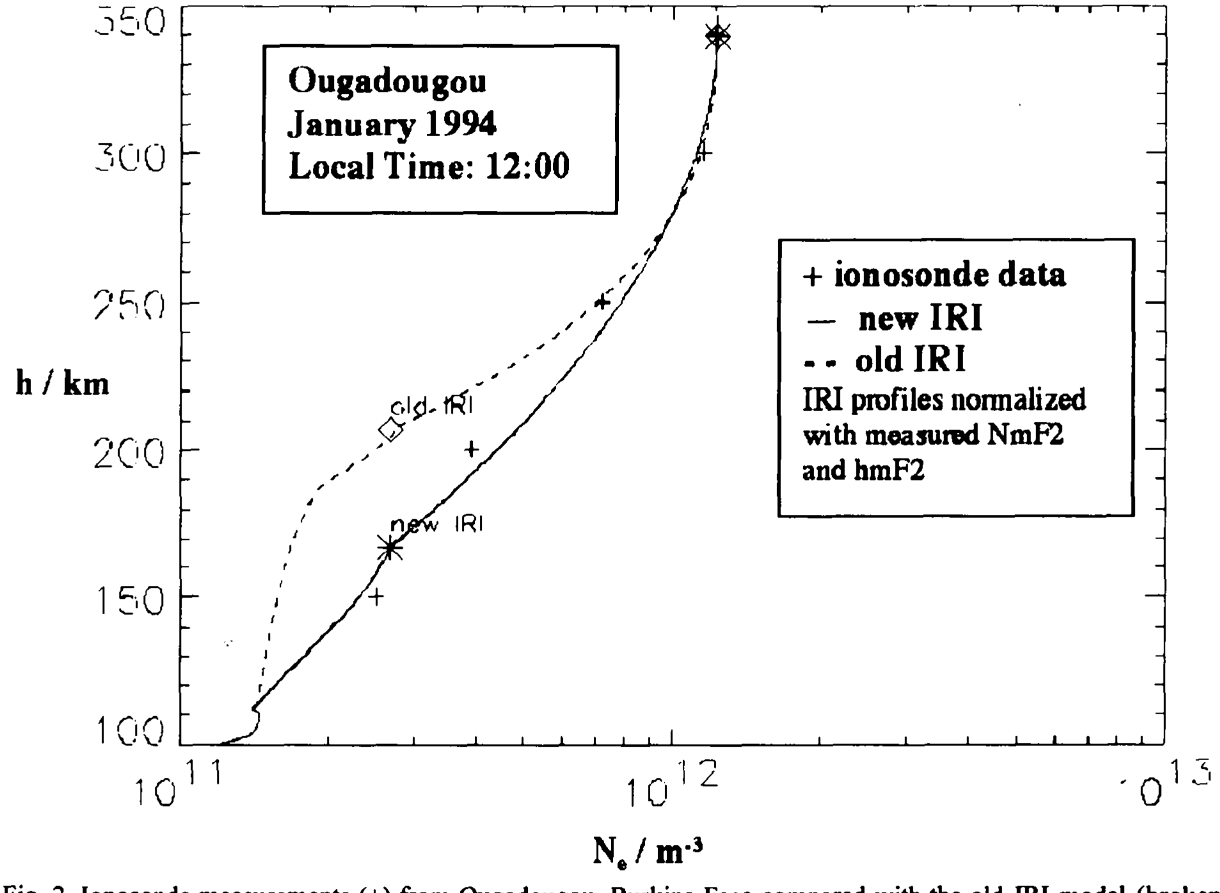

Fig. 2. Ionosonde measurements (+) from Ougadougou, Burkina Faso compared with the old IRI model (broken curve) and with the new IRI-2000 model (solid line). Also shown is the F1 point (asterisk and diamond).

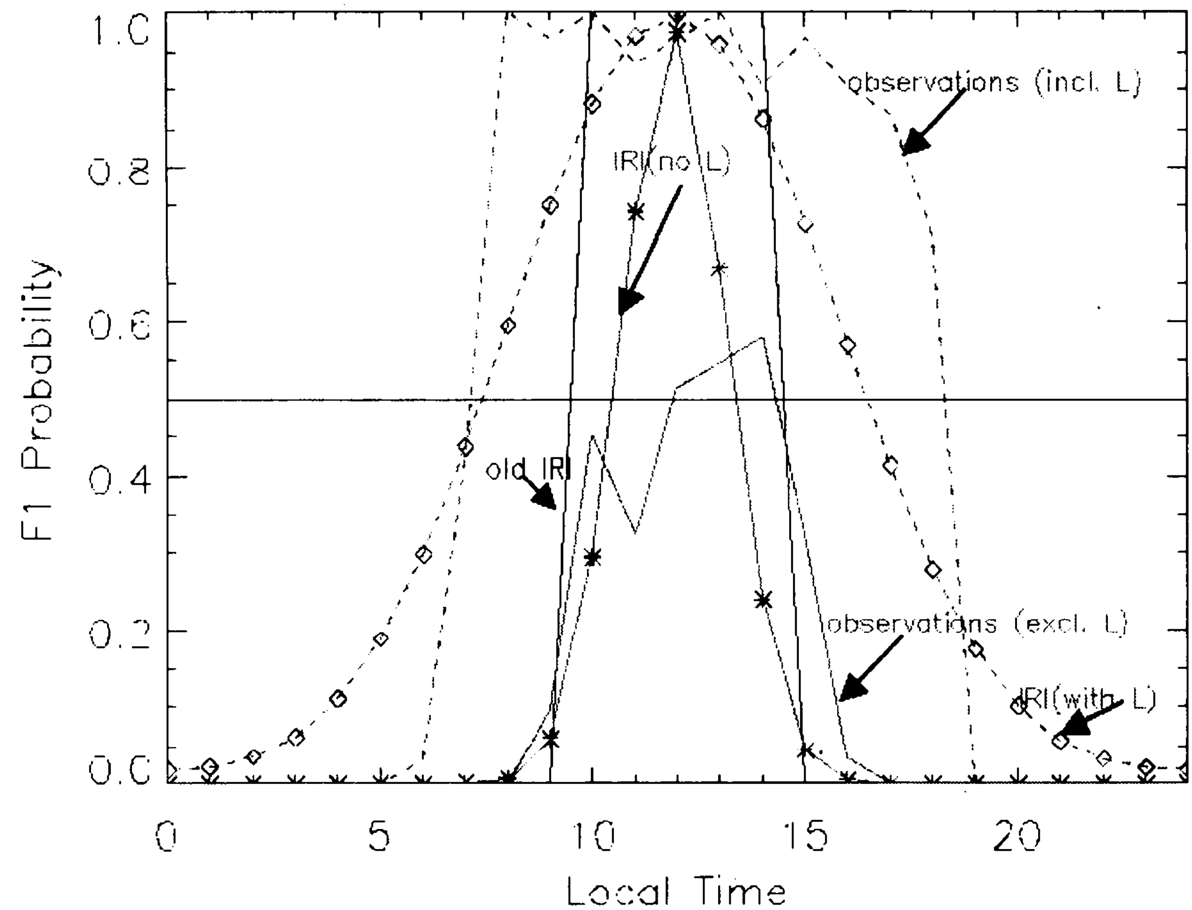

Fig. 3. F1 occurrence probability as measured at Tucuman in December 1979 excluding cases of L condition (solid curve) and including such cases (broken curve) compared with the IRI predictions without L (asterisk) and with L (diamonds) cases for summer during low solar activity. Also shown is the old (on-off) representation of F1 occurrence in previous IRI.

TABLE 1. New *B0* Table

Modip	R_{12}	*Spring*	*Spring*	*Summer*	*Summer*	*Fall*	*Fall*	*Winter*	*Winter*
degree	.	*LT=12*	*LT=0*	*LT=12*	*LT=0*	*LT=12*	*LT=0*	*LT=12*	*LT=0*
0	*10*	**201**	**68**	**210**	**61**	**192**	**68**	**199**	**67**
0	*100*	**240**	**80**	**245**	**83**	**233**	**71**	**230**	**65**
18	*10*	**108**	**65**	**142**	**81**	**110**	**68**	**77**	**75**
18	*100*	**124**	**98**	**164**	**100**	**120**	**94**	**96**	**112**
45	*10*	**78**	**81**	**94**	**84**	**81**	**81**	**65**	**70**
45	*100*	**102**	**87**	**127**	**91**	**109**	**88**	**81**	**78**

F1 OCCURRENCE PROBABILITY ADDED

As a new parameter IRI-2000 includes the probability for the occurrence of an F1 layer (percentage of days per month for which an F1 layer is expected). IRI uses the DuCharme et al (1971,1973) model that, on the basis of the long ionosonde data record, describes the F1 plasma frequency, foF1, in terms of solar zenith angle, magnetic latitude, and solar activity (R_{12}, 12-month running mean of sunspot number). The model also provides a criterion for the occurrence of an F1 layer by specifying the cutoff limiting solar zenith angle beyond which it cannot occur. This cutoff angle varies with R_{12} and magnetic latitude. A description of the variation of the F1 occurrence probability with solar zenith angle was recently developed by Scotto et al. (1997, 1998) based on the large volume of ionosonde data available from the US National Geophysical Data Center on the Ionospheric Digital Database CDs. They found that the IRI model described the measured foF1 values quite well but underestimated the time span (diurnal and seasonal) for which the F1 layer is observed. Their model describes the variations of the F1 occurrence probability (F1prob) in terms of solar zenith angle (χ), solar activity (R_{12}), and geomagnetic latitude ϕ

$$F1prob = (0.5 + 0.5 * \cos\chi)^{\gamma} \quad (4a)$$

$$\gamma = a = (b + c * \phi) * \phi \quad (4b)$$

$$a = 2.98 + 0.0854 * R_{12},\ b = 0.0107 - 0.0022 * R_{12},\ c = -0.000256 + 0.0000147 * R_{12} \quad (4c)$$

and provides a better match with the data. In addition it provides an option to include cases of L condition. Ionograms often exhibit a F1 ledge rather than a fully developed cusp, primarily during the time period just before the F1 layer disappears. These cases are described as L condition according to the URSI standard nomenclature. Scotto et al. (1997) find that if cases of L condition are included then an exponent $\gamma = 2.36$ can be used independent of latitude and solar activity. Both options (with and without L) are available for the IRI-2000 user. Figure 3 illustrates the diurnal variation of the F1 probability model in comparison with data from the ionosonde in Tucuman, Argentina. The figure also includes the old IRI model (on-off criterion), which clearly underestimates the probability of F1 occurrences if cases of L condition are included and overestimates the probability if such cases are excluded. The new probability function is closer to the observation but does not yet fully represent the diurnal structure of the data. This new parameter provides a continuous transition from F1 presence to non-presence and thus should be of help for especially for wave propagation studies.

NEW B0 AND B1 MODELS

The IRI electron density profile in the F2 bottomside is determined by a thickness parameter B_0 and a shape parameter B_1 (see Eq. (1)). IRI-2000 includes a new model for these parameters that is based on the analysis of a large volume of ionosonde data in the framework of the ICTP Task Force Activities (Bilitza et al., 2000). For B_0 a table of values was assembled for different latitudes, times of day, levels of solar activity, and seasons (Table 1). The most dramatic improvements are found near the magnetic equator, where the previous IRI B_0 model was based on extrapolations rather than data. Figure 4 compares the old and new B_0 model values with measurements from several equatorial ionosondes. The new B_0 values are about 30-40 % higher than the old ones and in better agreement with the data. For B_1 the TFA studies revealed a clear day-night difference and IRI-2000 uses the following average values:

$$B_1 = 1.9 \text{ nighttime},\ B_1 = 2.6 \text{ daytime} \quad (5)$$

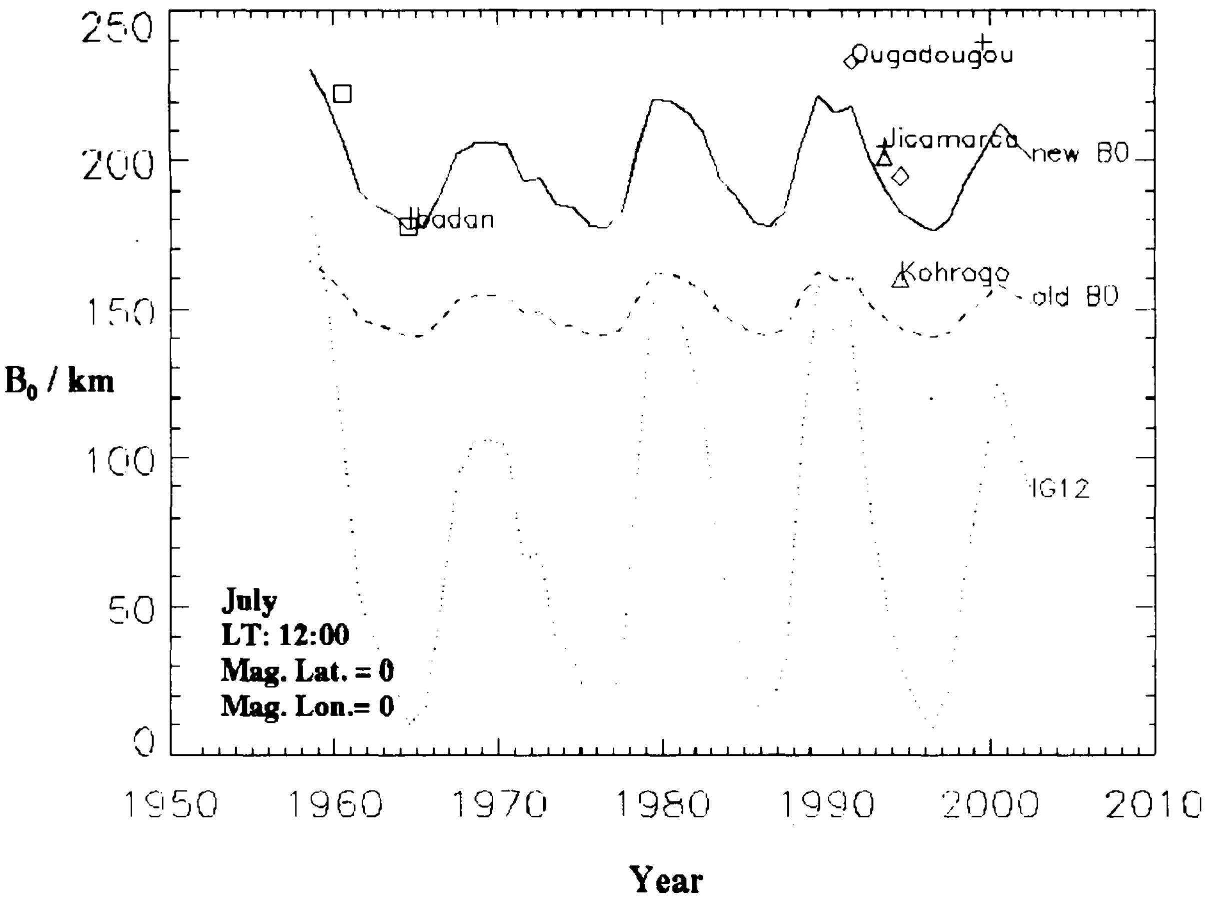

Fig. 4. Bottomside thickness parameter B0 as measured during summer noon at various equatorial ionosonde stations (symbols) and as predicted by the old (broken line) and new (solid line) IRI B0 models. Also shown is the IG12 ionospheric-effective solar index.

This reflects the difference in shape from the typical nighttime profile with a sharp drop into a deep nighttime valley compared to the gradual decrease during daytime down to first the F_1 layer and then a shallow E valley. The previous version of IRI assumed a constant value of $B_1 = 3$.

DESCRIPTION OF F PEAK STORM EFFECTS

The major change for the F peak density (NmF2) in IRI 2000 is the inclusion of a model for the description of the effects of magnetic storms on NmF2. The updating algorithm was developed by Fuller-Rowell et al. (1999, 2000) based on a large number of storms (in the time period 1980-1990) and their ionospheric response as seen by the worldwide ionosonde network. Their model captures the most obvious, long-lived, coherent feature of the ionospheric storm response, which is the deep ion depletion ("negative phase") that typically develops in the summer hemisphere during the driven phase of a storm and persists well into the recovery phase. The magnetic index applied is the integral of a_p over the previous 33 hours with a weighting function deduced from physically based modeling. Araujo-Pradere et al. (2002) have evaluated the IRI storm model with all the storms of 2000 and 2001 (14 in total) and the response seen at over 30 ionosonde stations. An example is shown in Figure 5. They find that during storm periods the IRI storm model provides a 30% improvement over the older IRI model and that IRI-2000 is able to capture more than 50% of the variability due to the storm.

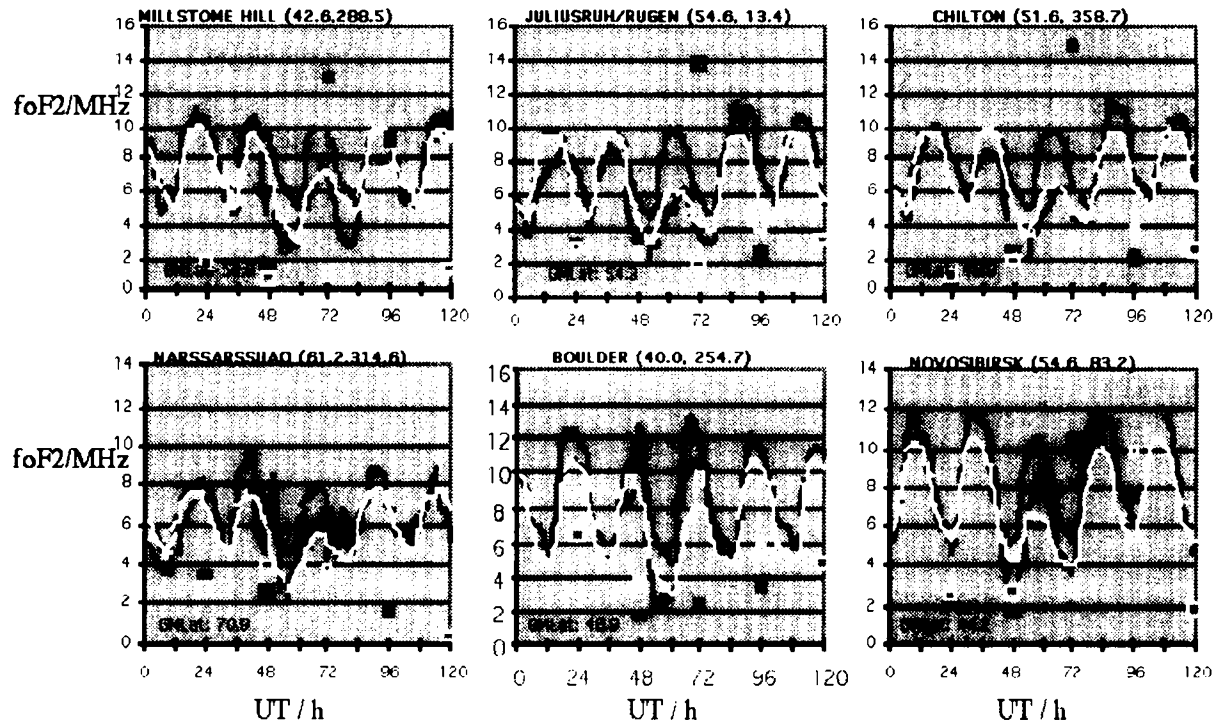

Fig. 5. foF2 as measured at several ionosonde stations during the April 5-9, 2000 storm (black line) and as predicted by IRI with storm model (white line) and without storm model (gray line) (Araujo-Pradere et al., 2002).

NEW OPTION FOR ELECTRON TEMPERATURE

As a major improvement the IRI-2000 electron temperature model now incorporates the height-specific models developed by Truhlik et al. (2000) and Triskova et al. (1996) based on data from three Intercosmos satellites. This will help to overcome shortcomings of the current IRI model in the description of the diurnal variation in the topside and help to overcome seasonal and solar cycle limitations of the earlier used database. The most notable changes are found in the upper topside, where the present model was limited to a simple day-night transition and did not reproduce the early morning and afternoon peaks seen in the satellite data (see example in Figure 6).

ION DRIFT FOR EQUATORIAL F REGION

A first ion drift model for IRI was developed by Kazimirovsky et al. (1990) using data obtained by ground-based radio techniques (D1, D3). Noting the considerable amount of ion drift data available from incoherent scatter radar stations and also from satellite in situ measurements, the IRI team has put high priority on including in IRI an ion drift model based on all the different data sources. As a first step, IRI 2000 will include the equatorial F region vertical drift model developed by Scherliess and Fejer (1999) based on radar and satellite data. Their model depends on local time, longitude, season, and solar activity and describes very well the characteristic diurnal features (maximum around noon and post-sunset pre-reversal spike) and their longitudinal, seasonal, and solar cycle differences. Inclusion of this model in IRI should be of help in the pursuit of a better understanding of the processes that shape the equatorial ionosphere and of the representation of this critical region in IRI. The pre-reversal peak in equatorial vertical drift results in a similar peak in the F peak height (hmF2). This feature is currently not reproduced

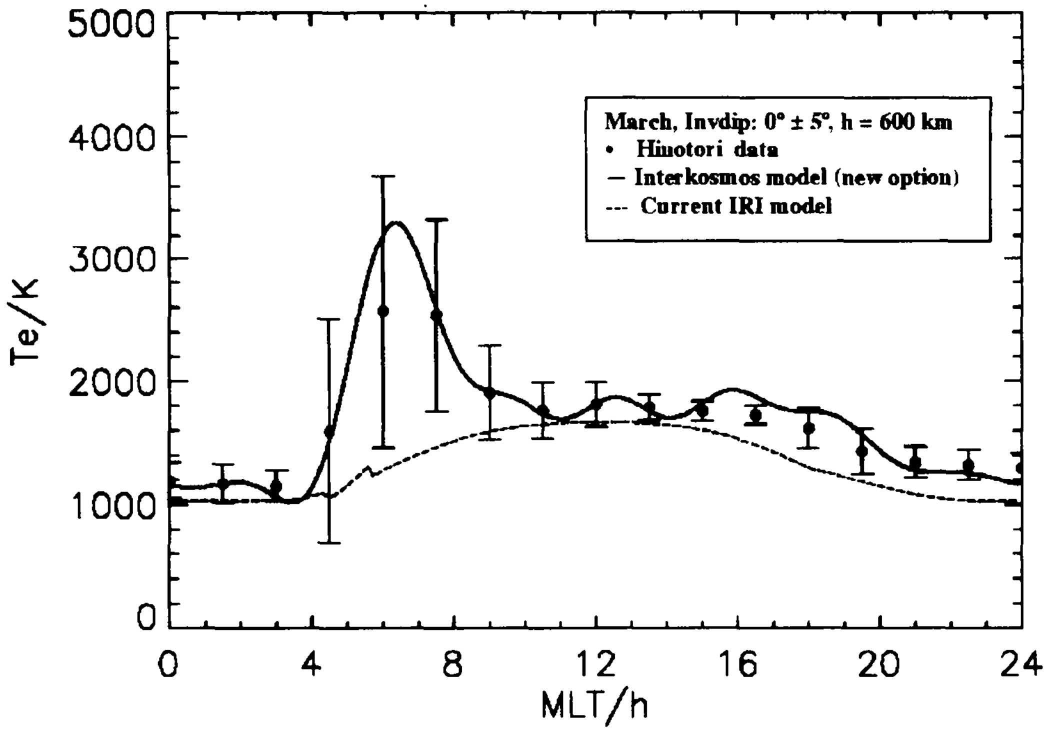

Fig. 6. The electron temperature at 600 km as measured by the Hinotori satellite and as predicted by the old IRI option (broken curve) and by the new Interkosmos model option (solid curve).

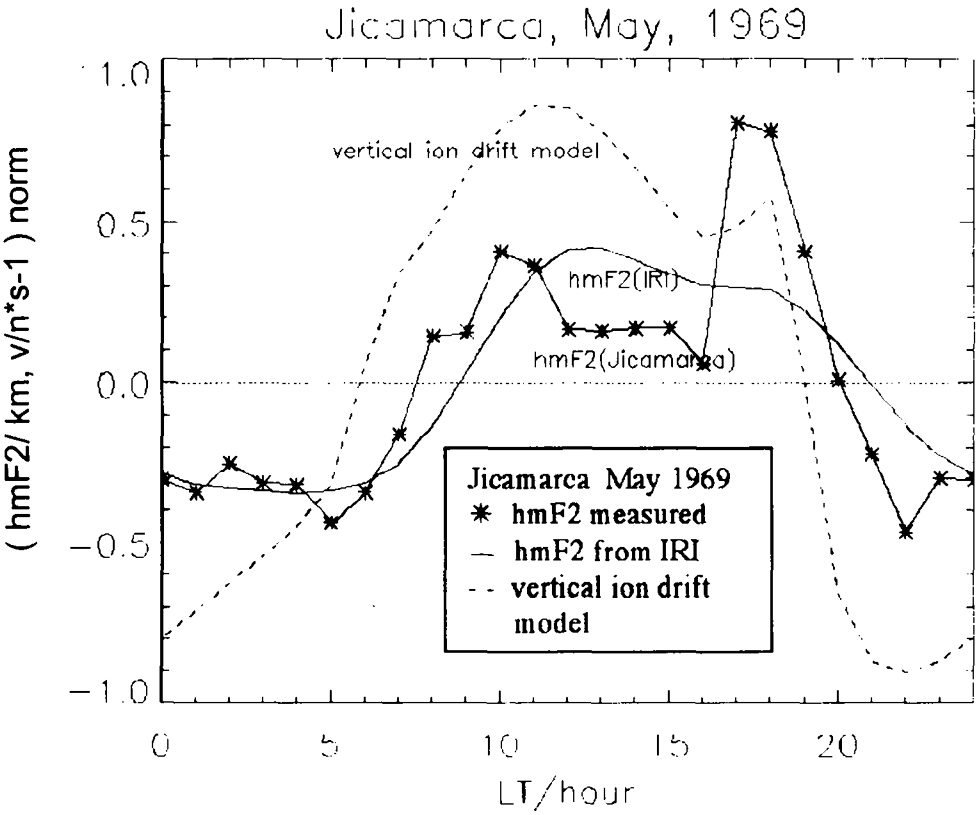

Fig. 7. The height of the F peak, hmF2, as measured at Jicamarca (asterisk) and hmF2 (solid curve) and equatorial vertical ion drift (broken curve) as predicted by the IRI model. All curves are normalized to comparable scales.

in the M3000-based IRI hmF2 model. A correlation with the new ion drift model may help to overcome this shortcoming. This is illustrated in Figure 7 with an example from Jicamarca.

CONCLUSION

The paper list and explains the most important changes introduced with the new version of the International Reference Ionosphere model, IRI-2000, and provides examples to illustrate these changes. The new version brings significant improvements of the electron density in the D-region, in the region from E valley to F2 peak, and at the peak during magnetic storm conditions. IRI-2000 includes a new option for the electron temperature which includes the morning overshoot also for the topside ionosphere. As new parameters IRI-2000 provides predictions for the F1 occurrence probability and for the vertical F-region ion drift at the magnetic equator.

ACKNOWLEDGMENTS

The author acknowledges the many, many individual efforts worldwide that have led to the significant improvements of the IRI model and that are now included in IRI-2000. The author's IRI work was partially supported through NSF grant ATM-9713469 and INT-0002144.

REFERENCES

Araujo-Pradere, E.A., T.J. Fuller-Rowell, and D. Bilitza, Comprehensive validation of the STROM response in IRI2000, submitted to *J. Geophys. Res.*, 2002.

Bilitza, D., Electron density in the *D*-region as given by the IRI, in *International Reference Ionosphere – IRI 79*, edited by V. Lincoln, R. Conkright, and K. Rawer, Rep. UAG-82, pp. 7-10, World Data Cent. A for Solar-Terrestrial Physics, Boulder, Colorado, Nov. 1981.

Bilitza, D., International Reference Ionosphere 2000, *Radio Sci.*, **36**(2), 261-275, 2001.

Bilitza, D., S. Radicella, B. Reinisch, J. Adeniyi, M. Mosert de Gonzalez, S. Zhang, and O. Obrou, New B_0 and B_1 models for IRI, *Adv. Space Res.*, **25**(1), 89-96, 2000.

Danilov, A., A. Rodevich, and N. Smirnova, Problems with incorporating a new D-region model into the IRI, *Adv. Space Res.*, **15**(2), 165-169, 1995.

DuCharme, E, L. Petrie, and R. Eyfrig, A method for predicting the F1-layer critical frequency, *Radio Sci.*, **6**, 369-378, 1971.

DuCharme, E, L. Petrie, and R. Eyfrig, A method for predicting the F1-layer critical frequency based on Zurich smoothed sunspot number, *Radio Sci.*, **8**, 837-839, 1973.

Friedrich, M., and K. Torkar, Typical behaviour of the high latitude lower ionosphere, *Adv. Space Res.*, **16**(1), 73-81, 1995.

Friedrich, M., and K. Torkar, Empirical D-region modelling, a progress report, *Adv. Space Res.*, **22**(6), 757-766, 1998.

Friedrich, M., R. Pilgram, and K. Torkar, A novel concept for empirical D-region modelling, *Adv. Space Res.*, **27**(1), 5-12, 2001.

Friedrich, and K. Torkar, FIRI: A semiempirical model of the lower ionosphere, *J. Geophys. Res.*, **106**, A10, 21409-21418, 2001.

Fuller-Rowell, T., M. Codrescu, E. Araujo-Pradere, and I. Kutiev, Progress in developing a storm-time ionospheric correction model, *Adv. Space Res.*, **22**(6), 821-827, 1999.

Fuller-Rowell, T., E. Araujo-Pradere, and M. Codrescu, An empirical ionospheric storm-time correction model, *Adv. Space Res.*, **25**(1), 139-148, 2000.

Kazimirovsky, E., E. Zhovty, and M. Chernigovskaya, Models for horizontal *E*- and *F*-region drifts, in *International Reference Ionosphere 1990*, Rep. 90-22, pp. 41-42, National Space Science Data Center, Greenbelt, Maryland, 1990.

Mechtley, E., and D. Bilitza, Models of *D*-region electron concentration, Rep. IPW-WB1, Institut für physikalische Weltraumforschung, Freiburg, Germany, 1974.

Radicella, S. (Ed.), *Proceedings of the IRI Task Force Activity 2000*, Abdus Salam International Centre for Theoretical Physics, Report IC/IR/2001/7, Trieste, Italy, 2001.

Radicella, S. (Ed.), *Proceedings of the IRI Task Force Activity 2002*, Abdus Salam International Centre for Theoretical Physics, Report IC/IR/2002/23, Trieste, Italy, 2002.

Radicella, S., D. Bilitza, B. Reinisch, J. Adeniyi, M. Mosert Gonzalez, B. Zolesi, M. Zhang, and S. Zhang, IRI task force activity at ICTP: proposed improvements for the IRI region below the peak, *Adv. Space Res.*, **22**(6), 731-739, 1998.

Rawer, K., D. Bilitza, and B. Reinisch (Eds.), International Reference Ionosphere – Workshop 1999, *Adv. Space Res.*, **27**(1), 1-180, 2001.

Rawer, K., D. Bilitza, and B. Reinisch (Eds.), Modelling the Topside Ionosphere and Plasmasphere, *Adv. Space Res.*, **29**(6), 805-1021 2002.

Reinisch, B. and X. Huang, Redefining the IRI F_1 Layer profile, *Adv. Space Res.*, **25**(1), 81-88, 1999.

Scherliess, L., and B. Fejer, Radar and satellite global equatorial *F* region vertical drift model, *J. Geophys. Res.*, **104**, 6829-6842, 1999.

Scotto, C., M. Mosert de Gonzalez, S. Radicella, and B. Zolesi, On the prediction of the F_1 ledge occurrence and critical frequency, *Adv. Space Res.*, **20**(9), 1773-1776, 1997.

Scotto, C., S. Radicella, and B. Zolesi, An improved probability function to predict the F_1 layer occurrence and L condition, *Radio Sci.*, **33**, 1763-1765, 1998.

Triskova, L., J. Smilauer, V. Truhlik, and V. Afonin, On the low latitude topside models: II electron temperature, *Adv. Space Res.*, **18**(6), 213-216, 1996.

Truhlik, V., L. Triskova, J. Smilauer and V. Afonin, Global empirical model of electron temperatures in the outer ionosphere for period of high solar activity based on data of three Intercosmos satellites, *Adv. Space Res.*, **25**(1), 163-172, 2000.